

Load Testing Application for Truss Bridge Design Verification: Dead Load Monitoring

Osman Hag-Elsafi¹; Jonathan Kunin²; and Sreenivas Alampalli^{3,*}

Submitted: 15 October 2024 Accepted: 11 December 2024 Publication date: 10 January 2025

DOI: 10.70465/ber.v2i1.14

Abstract: This is the first of two companion papers discussing the application of load testing techniques for the verification of bridge design. This truss bridge is atypical to conventional design, with the top chords of the main trusses, floor beams, and stringers designed to act composite with the concrete deck. Under load, in addition to axial forces, such a design creates secondary moments in the truss main members and complicates the analysis. This inspired the need for verification of the bridge design through instrumentation, monitoring, and load-testing program.

The objective of this paper is to verify the structural behavior of the bridge as designed under dead load. Achieving this objective required instrumentation of the main members of the erected structure and monitoring of strains in those members during concrete deck construction. For total dead load, a pseudo-analytical approach was used to incorporate load effects due to the self-weight of the structure. Five members of the downstream truss were instrumented with vibrating wire gages to record strains in those members during the first three deck pours. Finite element (FE) analysis and deck monitoring results were utilized in the pseudo-analytical approach to investigate actual axial forces and moments due to total service dead loads. The investigation indicated that measured forces and moments were within 20 percent of those estimated using FE analysis during the bridge design. The way the deck pours were accounted for in the design and the presence of construction loads on the deck during the monitoring might have contributed to this difference.

Author keywords: Load Testing; Bridge Evaluation; Bridge Analysis; Bridge Design; Nondestructive Testing; Structural Monitoring; High Performance Steel (HPS); Monitoring During Construction; Truss Bridge

Introduction

Conventional load testing of a bridge in good condition uses as-designed information and nominal material properties to investigate the response and behavior of the bridge under load and determine its load-carrying capacity. When a bridge ages and suffers from deterioration and section loss, load testing is the best option to investigate such parameters and estimate load-carrying capacity that reflects the bridge's in-service conditions. There are several examples of such testing in the literature.^{1-3,5-14} Besides such applications, load testing is also used by several others, including for verification of design assumptions. These are well documented in a recent state-of-the-practice paper¹ and load testing primer published by the Transportation Research Board.² These two references provide comprehensive literature, guidelines for testing, and how to execute the load test. Association

of American State Highway and Transportation Officials (AASHTO) is in the process of incorporating suggestions from the load testing primer into their load testing guidelines. Even though considerable literature exists on load testing, load testing and monitoring are accomplished in most cases for estimating live load stresses.

Instrumentation and load testing of existing bridges have been more widely used for diagnosing specific issues, evaluating load carrying capacity and assessing condition, evaluating structural response to loads, verifying the effectiveness of retrofits and materials, and monitoring for different purposes.^{1-3,5-14} Instrumentation during the construction of bridges has been less common (See References¹⁵⁻²¹ for sample studies). However, the future direction may hold a greater need for instrumentation during construction for health monitoring, even with the emergence of new technologies for the management of bridges, such as digital twin and non-contact sensors. Instrumentation during construction is unique in that it provides vital continuous information about a bridge's health throughout its cycles of construction, service life, and during adjacent ongoing construction activities.

This case study's contributions include estimating total dead load effects by monitoring strains in a limited number of truss members during staged deck construction, validating the unconventional design as a viable method for

*Corresponding Author: Sreenivas Alampalli.

Email: sreenivas.alampalli@stantec.com

¹New York State Department of Transportation (NYS DOT), Albany, NY 12232 (formerly with)

²New York State Department of Transportation, Albany, NY 12232

³Stantec, New York, NY, 10017

Discussion period open till six months from the publication date. Please submit separate discussion for each individual paper. This paper is a part of the Vol. 1 of the International Journal of Bridge Engineering, Management and Research (© BER), ISSN 3065-0569.

the structural design of truss bridges, and supplementing the limited literature on dead load monitoring of bridges.

Background and objectives

Instrumentation, strain monitoring, and load testing of a bridge in Tioga County, New York, are discussed in this and a companion paper. The bridge instrumentation, deck pour monitoring, and dead load analysis are discussed in this paper. The bridge structure and its design are also described in the paper. Load testing and live load analysis are the focus of the companion paper.⁴ For completeness, the paper also verifies the adequacy of the bridge structural design by considering both dead load and live load in the analysis.

The bridge replaced an old bridge and carries Route 96 (Court Street) over Route 17 and the Susquehanna River into the Village of Owego (Fig. 1). It has six spans (52, 65, 65, 65, 52, and 39 m) for a total length of 338 m. It is about 14.45 m wide, including a 12.40 m center-to-center spacing between two supporting trusses and two 1.02-m cantilever overhangs. It has three lanes of traffic, northbound, southbound, and a turning lane, and an Average Annual Daily Traffic (AADT) of about 6,000 vehicles at the time of the testing. The bridge is a continuous steel structure consisting of stringers, floor beams, two trusses (upstream and downstream), and a lightweight concrete deck. Some of the top and bottom chord members of the upstream and downstream trusses were made of High-Performance Steel (HPS). The concrete deck was built as a composite with the stringers as well as the top chords of the trusses. The fact that the deck is composite with the top chords of the trusses generally introduces secondary moments in the truss members and complicates structural behavior. Moments in the truss members are also influenced by the behavior of the bolted connections, acting as pinned, semirigid, or rigid.



Figure 1. Court street bridge

The project was initiated to investigate axial forces and moments in the main truss members due to service deck dead load and service live loads, to verify the unconventional design. Five carefully selected members of the downstream truss were instrumented with vibrating wire gages to record strains in those members during the first three deck pours and to collect additional data during a load test conducted after the bridge construction was completed. The instrumented members were located near Pier 1 side of Span 2 on the downstream truss (Spans 1 and 2, respectively, are shown in Figs. 2 and 3, and Pier 1 is shown in both figures).



Figure 2. Span 1 downstream view



Figure 3. Span 2 downstream view

For the instrumented members, this and the companion paper present relationships between the design service loads axial forces and moments (based on FE analysis results) and the actual axial forces and moments (based on monitoring and load test results).

Paper organization

The above section gave details of the bridge and the objectives of the testing. The following section describes the bridge analysis and design related to dead load, followed by details of the instrumentation and deck load monitoring plans. Collected deck pour monitoring data is then analyzed and compared with the finite element analysis results. Plots for predicting actual service load axial forces and moments due to dead load in the instrumented members are then derived. The paper concludes with closing remarks.

Analysis and Design of the Bridge Structure

Bridge analysis

The structure was analyzed using the New York State Department of Transportation (NYSDOT) approved computer program at the time for truss analysis and rating (BLRS) and a general structural analysis finite element program STAAD III.

Bridge design

The bridge was designed based on the New York State Department of Transportation approved specifications and standards for highway bridges with all provisions in effect

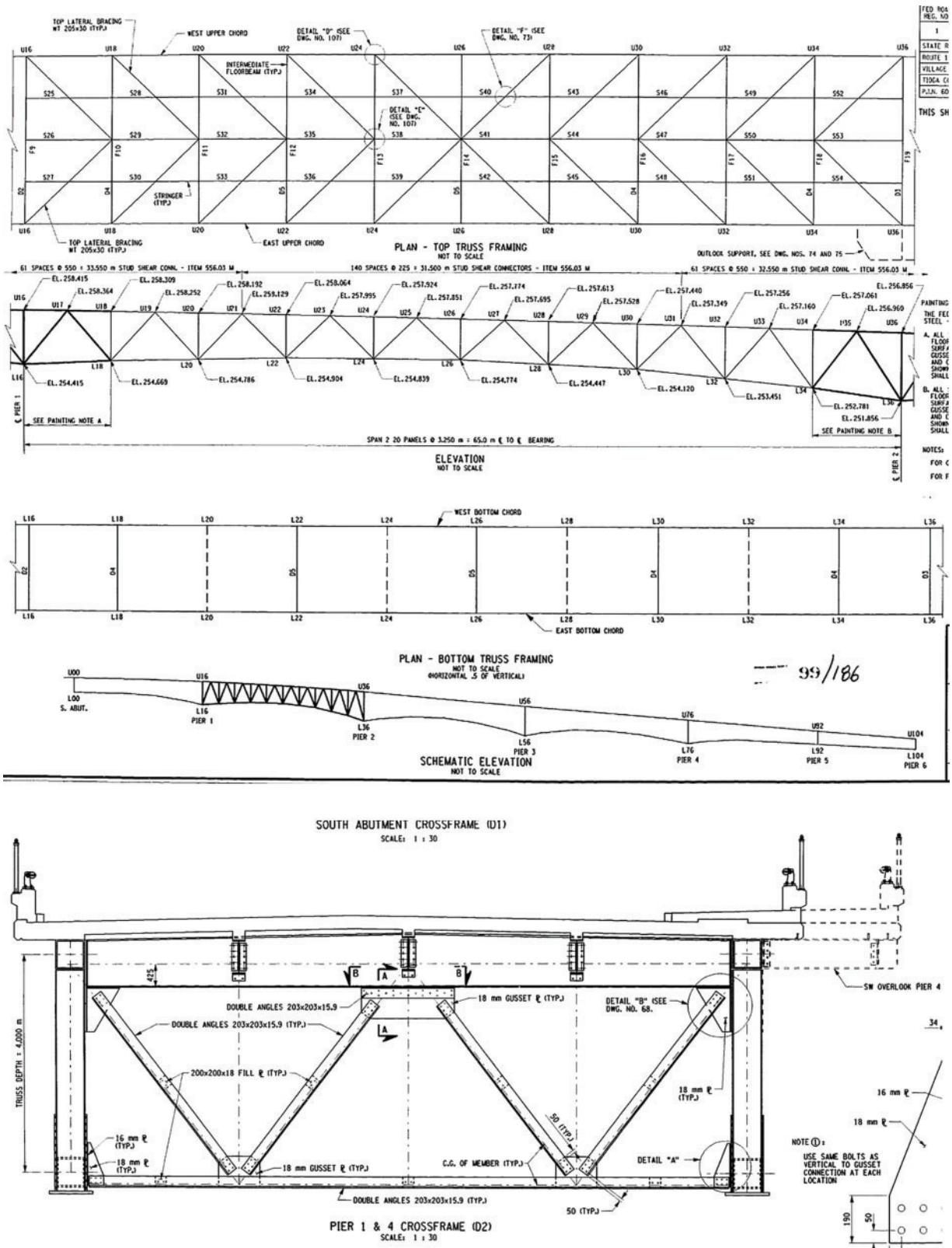


Figure 4. Span 2 framing plan and cross frames

during the testing that included AASHTO Standard Specifications for Highway Bridges, 16th edition and interims, AASHTO Guide Specifications for Strength Design of Truss Bridges and interims. ²²⁻²⁶

The bridge superstructure steel conforms to ASTM A709M Grade 345 W (non-HPS) or ASTM A709M Grade 485 W (HPS). An elastic modulus of 2×10^5 MPa was specified for the design of both steel-type members. ²⁶

Table 1. Members shapes shape and steel grades

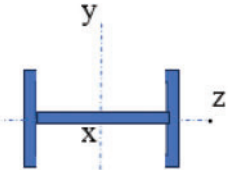
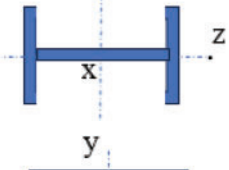
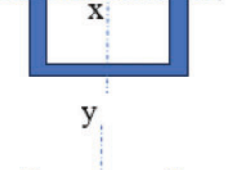
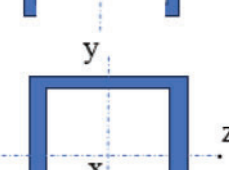
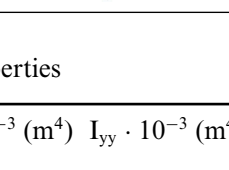
Gage number	Member mounted on	Section	Length (mm)		Thickness (mm)		Steel grade	F_y (MPa)
			Web	Flange	Web	Flange		
1	U16-L16		533	270	10	14	345 W	345
2	U16-L16							
3	L16-U17		533	433	14	30	345 W	345
4	L16-U17							
5	L16-L18		533	533	28	18	485 W	485
6	L16-L18							
7	L16-L18							
8	L16-L18							
9	U17-L18		533	473	10	28	345 W	345
10	U17-L18							
11	U16-U17		533	533	38	20	485 W	485
12	U16-U17							

Table 2. Instrumented members' properties

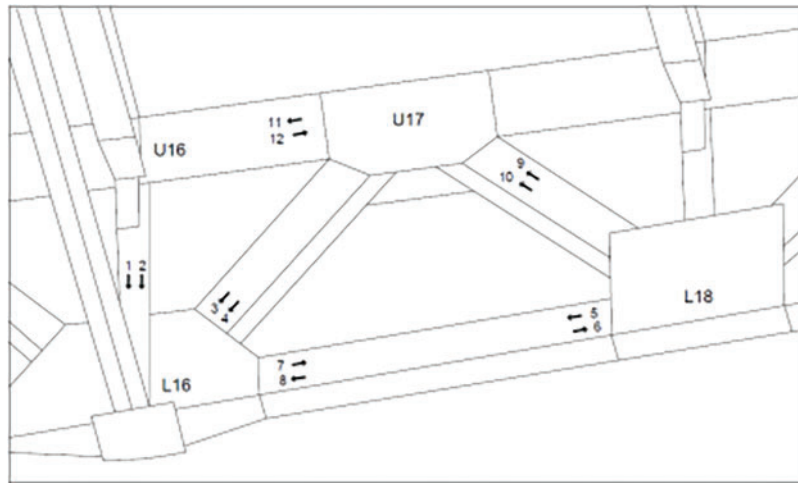
Member	Length (m)	Gross area (m ²)	$I_{zz} \cdot 10^{-3}$ (m ⁴)	$I_{yy} \cdot 10^{-3}$ (m ⁴)	$S_z \cdot 10^{-3}$ (m ³)	$S_y \cdot 10^{-3}$ (m ³)	$r_z \cdot 10^{-1}$ (m)	$r_y \cdot 10^{-3}$ (m)	L/r
U16-L16	4.00	0.0126	0.05	0.62	0.34	2.44	2.21	0.60	66.25
L16-U17	5.15	0.031	0.32	1.64	1.60	6.49	2.32	1.02	50.02
L16-L18	6.52	0.0470	1.61	2.22	7.16	8.79	2.26	1.92	33.82
U17-L18	4.88	0.0255	0.24	1.41	1.18	5.60	2.35	0.96	51.09
U16-U17	3.25	0.0588	2.16	2.80	8.10	12.6	2.26	1.86	17.46

The framing plan and cross frames for Span 2 are shown in Fig. 4. The instrumented members' shapes, web, and flange dimensions, steel grades, and yield stresses (F_y) are presented in Table 1. The members' properties [moment of inertia (I), section modulus (S), radius of gyration (r), and length (L) over radius of gyration ratio (L/r)] are given in Table 2. To avoid unnecessary repetition when discussing the

instrumentation plan, the gage numbers mounted on the respective truss members are also shown in Tables 1 and 2. For design purposes, compressive strength and elastic modulus of concrete for the substructure and deck slab at 28 days were also specified at 21 days (1.64×10^4 MPa). Service dead load axial forces and moments used for the bridge design are included in Table 3.

Table 3. Service dead load axial forces and moments

Gage number	Member mounted on	Dead load	
		Axial force (kN)	Secondary moment (kN-m)
1, 2	U16-L16	-343	1
3, 4	L16-U17	-2291	38
5, 6, 7, 8	L16-L18	-5120	241
9, 10	U17-L18	1931	22
11, 12	U16-U17	6423	267

**Figure 5.** Instrumented downstream truss members**Table 4.** Gage locations on members

Gage number	Member mounted on	Distance from starting member's end (m)
1	U16-L16	1.41
2	U16-L16	1.41
3	L16-U17	1.58
4	L16-U17	1.58
5	L16-L18	5.30
6	L16-L18	5.30
7	L16-L18	1.64
8	L16-L18	1.64
9	U17-L18	1.46
10	U17-L18	1.46
11	U16-U17	1.35
12	U16-U17	1.35

Instrumentation and Load Test Plans

The bridge instrumentation plan was designed to provide data for the investigation of axial forces and secondary moments in the downstream truss members. The gages were mounted in pairs near member ends to collect strain and temperature data during the first three deck pours and for a post-construction load test. Vibrating wire gages (Geokon

Model 4000) were used for their long-term durability and not requiring correction for drift. The gages were read using a Geokon Model GK-403 readout box, which reads one gage at a time, giving the gage's strain in $\mu\epsilon$ and temperature in $^{\circ}\text{C}$. The vibrating wire gages have a Gage Correction Factor of 0.945.

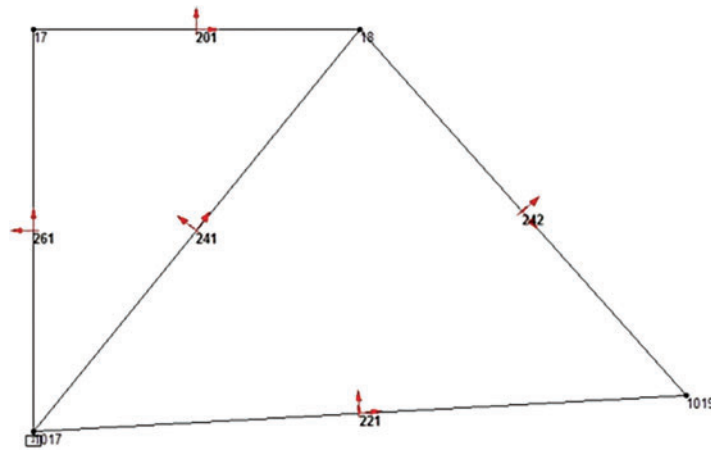


Figure 6. Member local axis orientation

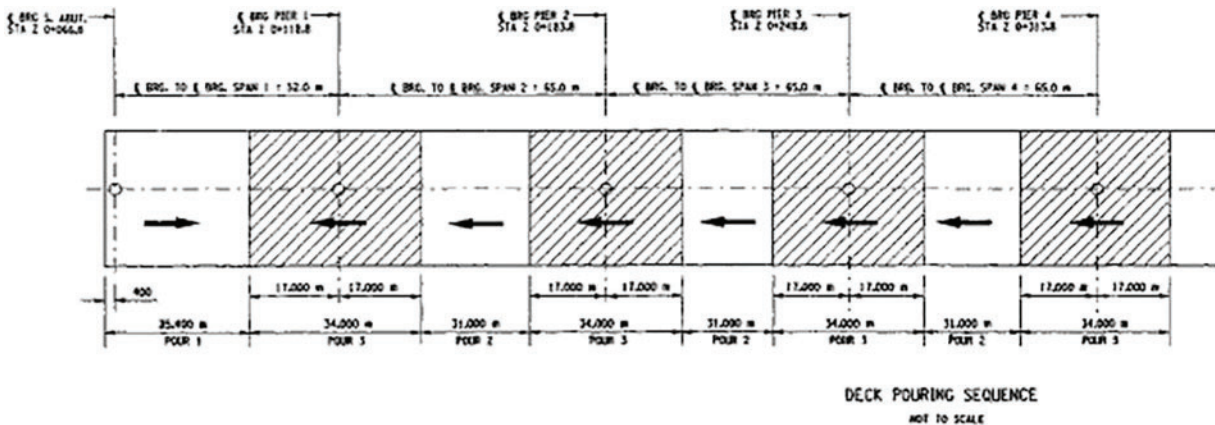


Figure 7. Deck pour sequence

Instrumentation

The five members selected for instrumentation were located near Pier 1, at the end of Span 2 (Figs. 2, 3, and 5) of the downstream truss. All gages were arc-welded to the members, except for the top chord (U16-U17) where they were mounted using a quick set epoxy resin. The gage locations along the members are shown in Table 4, where the starting ends are defined based on the local member axes coordinate systems in Fig. 6. In the transverse directions, all the gages were mounted 13 mm from a member's nearest edge, except for Gage 11 which was mounted 35 mm below the edge next to the concrete deck. All the gages remained operational throughout the project, except for the two gages mounted on the top chord (Gages 11 and 12), which debonded before the live load tests were performed.

Monitoring Results and Dead Load Analysis

Monitoring results

Strain data was collected for deck Pours 1, 2, and 3 (see Fig. 7) during October and November 2002. There was a pause in construction activities during the winter season before the rest of the deck was cast. The average temperature

changes during Pours 1, 2, and 3 were 8.7, 12.4, and 2.3°C, respectively. The strain and temperature data collected during the three deck pours is documented in an NYSDOT report (Hag-Elsafi, Kunin, and Alampalli 2006).³ The strain data was corrected for temperature effects and a summary of the corrected strains and stresses for the three pours is given in Table 5.

Time histories of the stresses calculated for each paired gage on a member during the three pours are presented in Fig. 8. The horizontal axes in these plots are indicative of selected areas of the deck being poured and the corresponding pour numbers. The plots in the figure show the general quantitative changes in a gage's stress as the deck is poured in the direction (beginning-to-end) depicted by the arrows in Fig. 7. The stress histories in the figure were calculated using corrected strain data, as shown in the last column in Table 5.

The time history plots in the figure are generally consistent with the influence line plots (Appendix B of Hag-Elsafi, Kunin, and Alampalli, 2006),³ regarding the effect of a poured deck area on a member's axial force. The plots also show the bending experienced by the members during the three deck pours, which is indicated by the separation between the two time-history lines for any paired gages mounted on a member. Based on this data, it can be concluded that members U16-U17 (top chord) and L16-L18

Table 5. Deck pours strains and stresses

Gage	Member	Pours 1 + 2 + 3 temperature corrected strain ($\mu\epsilon$)	Pours 1 + 2 + 3 temperature-corrected strain w/gage factor ($\mu\epsilon$)	Total stress (MPa)
1	U16-L16	-167.5	-158.3	-31.7
2	U16-L16	-191.4	-180.8	-36.2
3	L16-U17	-233.1	-220.3	-44.1
4	L16-U17	-213.4	-201.6	-40.3
5	L16-L18	-284.6	-268.9	-53.8
6	L16-L18	-265.6	-251.0	-50.2
7	L16-L18	-200.3	-189.3	-37.9
8	L16-L18	-338.6	-320.0	-64.0
9	U17-L18	175.5	165.9	33.2
10	U17-L18	269.5	254.7	50.9
11	U16-U17	224.8	212.4	42.5
12	U16-U17	117.6	111.1	22.2

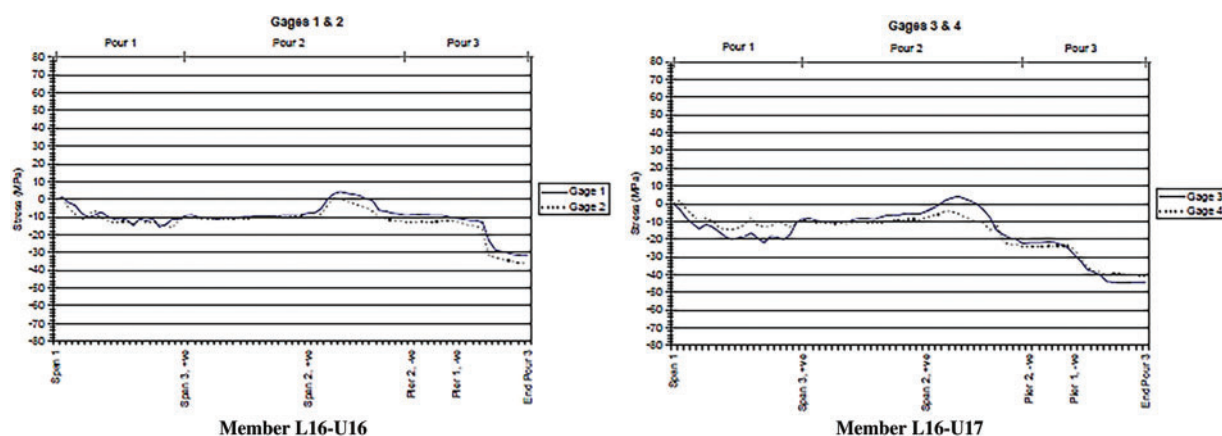
Table 6. Deck load axial forces and secondary moments

Gage number	Member mounted on	Axial force (kN)		Secondary moment (kN-m)	
		FE	Test	FE	Test
1, 2	U16-L16	-175	-428	1	6
3, 4	L16-U17	-1068	-1291	21	12
5, 6	L16-L18	-2581	-2444	137	115
7, 8	L16-L18	-2581	-2394	137	115
9, 10	U17-L18	1074	1072	12	50
11, 12	U16-U17	3258	1903	150	128

(bottom chord) are the two most stressed members, as expected, and member strains are mostly influenced by deck pours on Span 2, positive moment region of the span and negative regions at Piers 1 and 2. From the strain data in the figure, the highest tensile and compressive forces, and end moment in the members can be calculated as follows:

The highest tensile force resulted in the top chord = (average strain for Gages 11 and 12) \times steel elastic modulus \times top chord area = $162 (\mu\epsilon) 2 \times 1011 (\text{Pa}) \times 58.8 \times 10^{-3} (\text{m}^2) = 1,903 \text{ kN}$.

The highest compressive force resulted in the bottom chord = (average strain for Gages 5 and 6) \times steel elastic

**Figure 8.** (Continued)

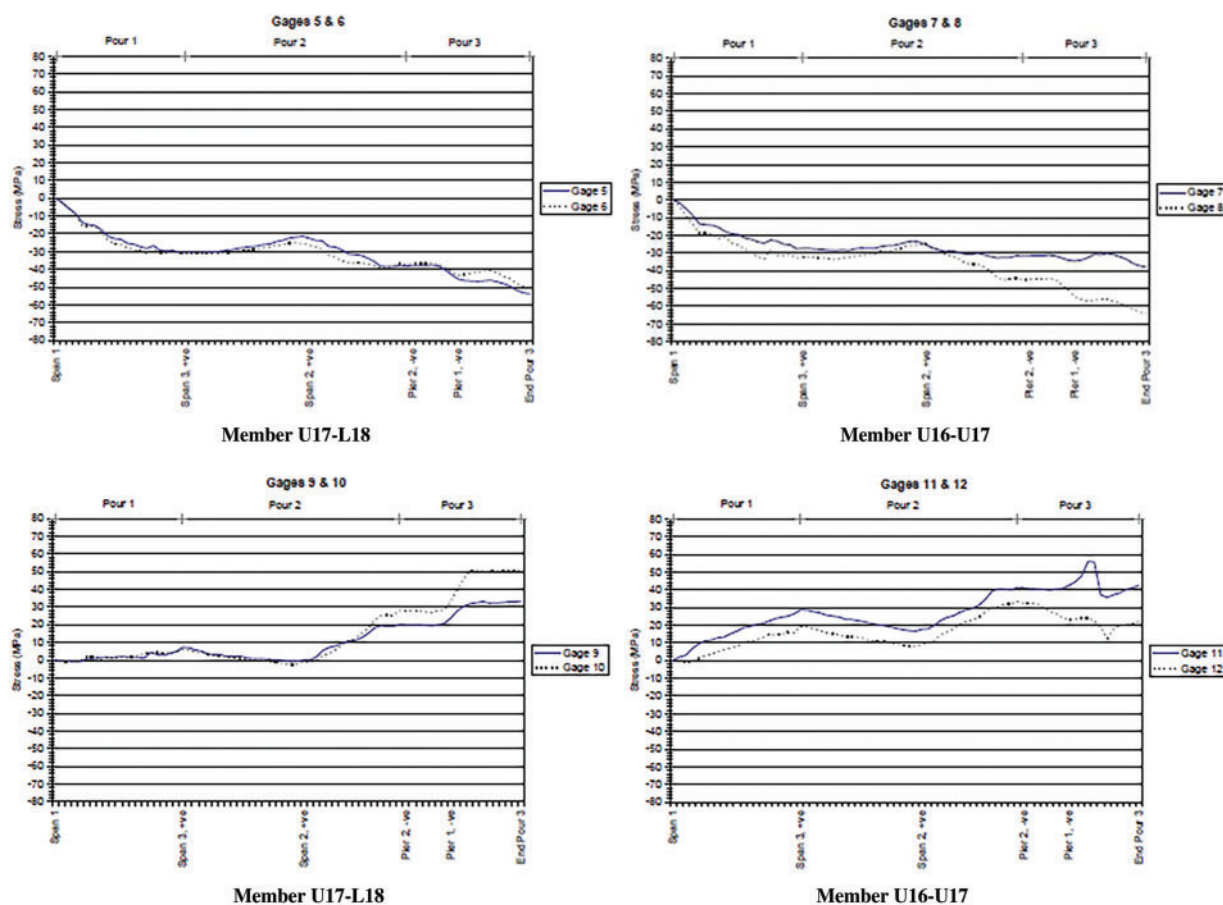


Figure 8. Deck pour stresses for paired gages

modulus \times bottom chord area = $260 (\mu\epsilon) 2 \times 10^{11} (\text{Pa}) \times 47.0 \times 10^{-3} (\text{m}^2) = 2,444 \text{ kN}$.

Both the highest compressive and tensile forces were calculated based on the strains recorded at the end of Pour 3. The highest bending moment resulted in the top chord when the deck area directly above Pier 1 was poured = $(1/2 \text{ strain difference for Gages 11 and 12}) \times \text{steel elastic modulus} \times \text{bottom chord section modulus} = 1/2 \times 101 (\mu\epsilon) 2 \times 10^{11} (\text{Pa}) \times 12.6 \times 10^{-3} (\text{m}^3) = 128 \text{ kN}\cdot\text{m}$.

This is a predictable consequence of the deck being cast to act composite with the top chord members.

To determine axial forces and moments in the truss members due to service deck load, the total stresses in Table 5 were split into their axial and bending stress components. Stress measured at a gage location generally represents the net contribution of the individual stresses due to axial forces, bending about the y and z-axes, and torsion (bending about the x-axis). From a three-dimensional FE deck load analysis results, stresses due to bending about the y-axis and torsion on the truss members were found to be relatively small in comparison to those due to axial forces and bending about the z-axis. As such, the axial stress on the member could be obtained as the average of the stresses calculated based on the two paired-gages readings multiplied by the member's cross-sectional area and the bending stress due to secondary moments (M_z , bending about the z-axis) as half

the difference between the two calculated axial stresses times the member's section modulus.

Axial forces and secondary moments for the FE analysis and monitoring results are included in Table 6 and presented in Figs. 9 and 10. The graphical presentation in these figures establishes a relationship between the test (actual) and FE analysis results for axial forces (Fig. 9) and moments (Fig. 10). The fact that these relationships are linear illustrates the consistency of the test data and the linear behavior of the structure.

Based on the results from a two-dimensional FE analysis, used for the bridge design, the concrete deck load effects were determined to be about 65 percent of the total service dead load effects. The FE analysis dead load, secondary moments in Table 6, were obtained by proportioning those shown on the bridge plans by the 65 percent factor and adjusting for the lightweight concrete deck. Incremental FE analysis results (Tables 7A to 7C) of the structure considering the actual deck pouring sequence confirmed the validity of the above approach to estimate concrete deck axial forces and moments. This is demonstrated by the excellent comparison between the FE and proposed approach results in Table 7D. The incremental FE analysis was performed, ignoring the composite action provided by the cured concrete during the deck pours. Besides axial forces (F_x) and bending moments about the z-axis (M_z), Table 7 shows additional results from the FE analysis, including shear

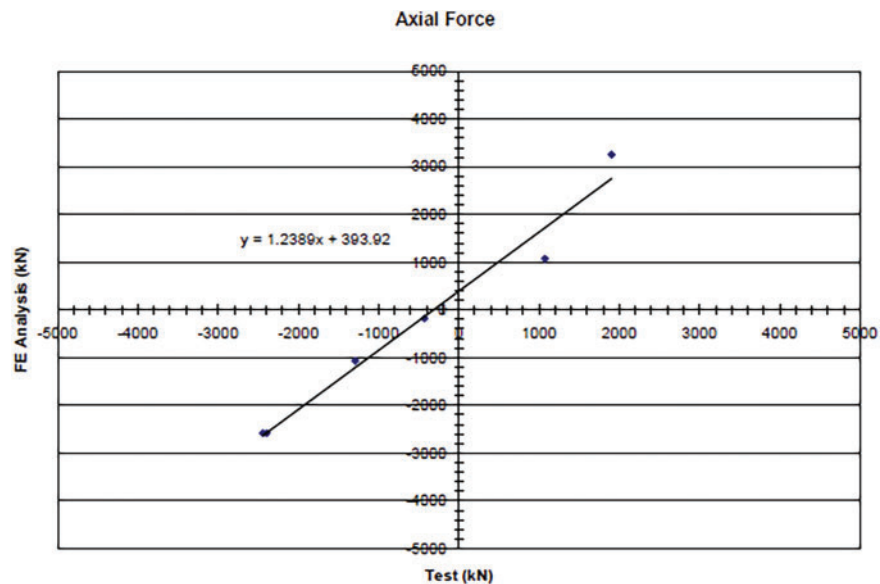


Figure 9. Axial force (F_A): deck service load (FE Analysis) versus load test

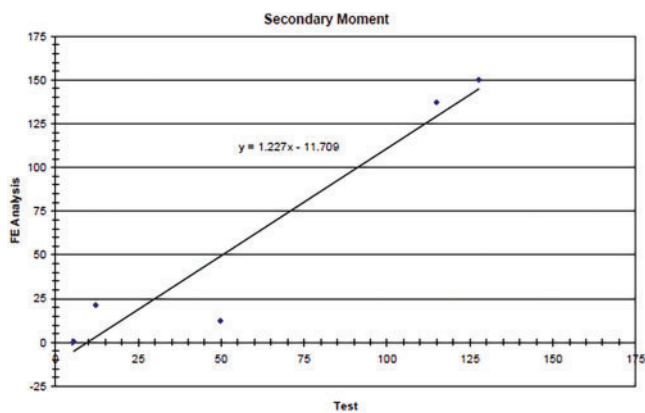


Figure 10. Bending moment (M_z): service deck load (FE Analysis) versus load test

forces (F_y and F_z), out-of-plane bending moments (M_y), and torsional forces (M_x). The unpredictable out-of-plane bending results in [Table 8](#) clearly show the importance of three-dimensional FE analysis in investigating the structural behavior of bridges designed in a similar manner to that discussed in this paper.

Dead load analysis

The goal of this section is to determine axial forces and secondary moments in the instrumented members under total service dead load using the service deck load analysis results. This was achieved by applying the 65 percent factor to the FE and monitoring results in [Table 6](#) to generate a similar set of data for predicting total service dead load axial forces and moments. This new data set is shown in [Table 8](#) and graphically displayed in [Figs. 11](#) and [12](#). Analyses of the data sets used to generate these figures (see Appendix D of Hag-Elsafi, Kunin, and Alampalli, 2006) show the statistical significance of the relationships between FE and test results established in the figures.

It is important to note that the above approach for predicting total dead load effects is based on the assumptions that 1) structural characteristics of the bridge were not affected by the concrete curing process, and the subsequent loss of moisture and the possibility of the poured concrete acting compositely with the steel, 2) temperature changes between concrete pours were uniform (this was used in the calculation of the Thermal Gage Factors, TGFs, supplied with the strain gages), and 3) the deck load was applied incrementally, a manner resembling actual pours sequence, in the FE solution for forces and moments due to the deck pours.

Table 7. Finite element analysis results for the first three-deck pours and summary

Member	Element no.	Node no.	F _x (kN)	F _y (kN)	F _z (kN)	M _x (kN-m)	M _y (kN-m)	M _z (kN-m)
A. Pour 1 results								
U16-L16	261	1017	20.8	0.4	0.1	0.0	-0.1	0.8
		17	-20.8	-0.4	-0.1	0.0	-0.5	1.0
L16-U17	241	1017	35.8	0.0	0.4	0.0	-0.7	3.2
		18	-35.8	0.0	-0.4	0.0	-1.4	-3.2
L16-L18	221	1017	1227.9	2.0	-0.1	-0.1	0.4	31.8
		1019	-1227.9	-2.0	0.1	0.1	0.4	-18.7
U17-L18	242	18	-43.6	0.0	0.1	0.0	-0.6	1.9
		1019	43.6	0.0	-0.1	0.0	0.3	-1.7
U16-U17	201	17	-1169.7	7.3	-2.1	0.6	9.3	51.6
		18	1169.7	-7.3	2.1	-0.6	-2.4	-27.8
B. Pour 2 results								
U16-L16	261	1017	17.1	-0.5	0.1	0.0	-0.1	-0.9
		17	-17.1	0.5	-0.1	0.0	-0.4	-1.1
L16-U17	241	1017	472.4	-1.4	0.1	0.0	-0.3	-0.5
		18	-472.4	1.4	-0.1	0.0	-0.3	-6.7
L16-L18	221	1017	728.1	6.9	0.3	-0.8	-3.2	42.1
		1019	-728.1	-6.9	-0.3	0.8	1.5	2.7
U17-L18	242	18	-495.2	-2.0	-0.6	0.0	0.4	-3.8
		1019	495.2	2.0	0.6	0.0	2.6	-5.7
U16-U17	201	17	-971.6	8.6	2.7	-0.6	-11.0	42.7
		18	971.6	-8.6	-2.7	0.6	2.3	-14.7
C. Pour 3 results								
U16-L16	261	1017	173.6	0.0	7.6	0.0	-5.8	0.0
		17	-173.6	0.0	-7.6	0.0	-24.4	0.0
L16-U17	241	1017	502.3	-0.7	5.7	0.0	-3.0	1.9
		18	-502.3	0.7	-5.7	0.0	-26.5	-5.3
L16-L18	221	1017	553.6	10.3	2.1	-4.1	-15.0	51.5
		1019	-553.6	-10.3	-2.1	4.1	1.5	15.6
U17-L18	242	18	-427.7	-2.1	-3.0	0.0	8.9	-4.8
		1019	427.7	2.1	3.0	0.0	5.7	-5.4
U16-U17	201	17	-833.4	-2.7	-6.0	4.5	8.0	34.2
		18	833.4	2.7	6.0	-4.5	11.6	-42.9
D. Summary and comparison with the proposed approach in Table 7								
Member	Element no.	Node no.	FE results pours 1 + 2 + 3		Proposed approach			
			F _x (kN)	M _z (kN-m)	F _x (kN)	M _z (kN-m)		
U16-L16	261	1017	211.5	-0.2	-175	1		
		17	-211.5	-0.1				
L16-U17	241	1017	1010.5	4.5	-1068	21		
		18	-11010	-15.2				
L16-L18	221	1017	2509.6	125.3	-2581	137		
		1019	-2509.0	-0.4				
U17-L18	242	18	-966.5	-6.7	1074	12		
		1019	966.5	-12.8				
U16-U17	201	17	-2974.7	128.4	3258	128		
		18	2974.7	-85.4				

Table 8. Total dead load axial forces and secondary moments

Gage number	Member mounted on	Axial force (kN)		Secondary moment (kN-m)	
		FE	Test	FE	Test
1, 2	U16-L16	-267	-658	1	9
3, 4	L16-U17	-1672	-1987	33	19
5, 6	L16-L18	-3962	-3759	-	-
7, 8	L16-L18	-3962	-3683	212	177
9, 10	U17-L18	1642	1650	19	76
11, 12	U16-U17	5022	2927	231	196

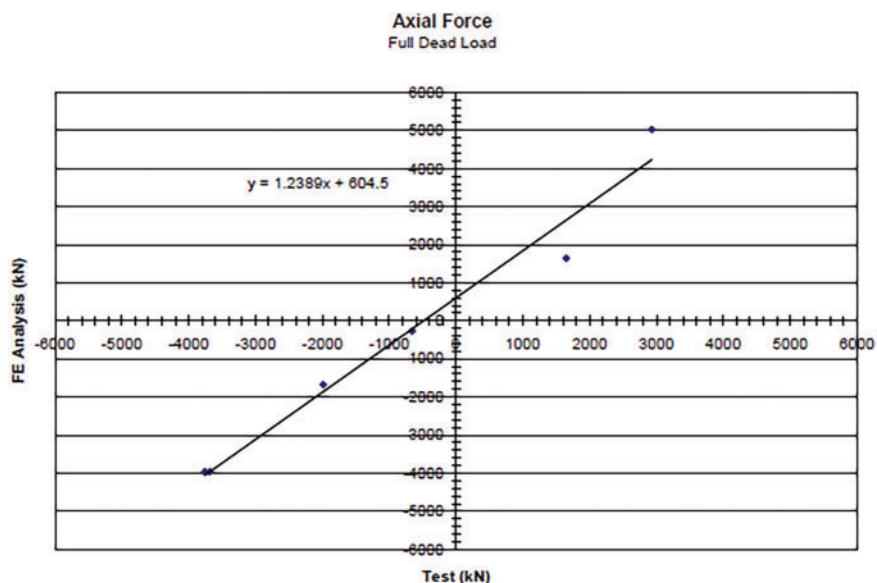


Figure 11. Axial force (F_A): service total dead load (FE Analysis) versus load test

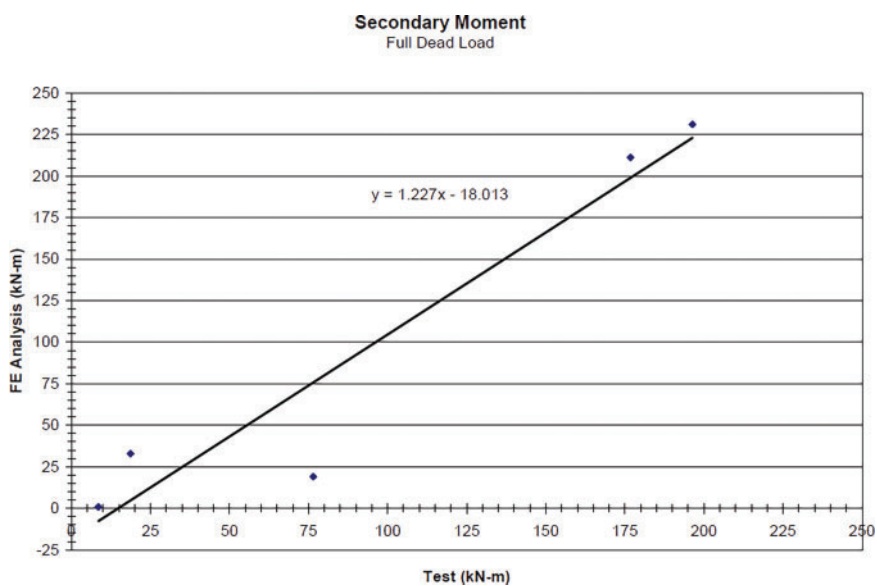


Figure 12. Bending moment (M_z): service dead load (FE Analysis) versus load test

Conclusions

Instrumentation and deck pour monitoring of a truss bridge with the top chords of the main trusses, floor beams, and stringers designed to act composite with the concrete deck were discussed in this paper. The bridge is a six-span continuous steel structure about 338 m long and 14.45 m wide. The objective of the project was to determine service dead load axial forces and secondary moments in the bridge truss members as verification of the unconventional design of the structure. Vibrating wire gages were mounted on five members of the downstream truss to record strains in those members during the first three deck pours.

Based on the data, it was concluded that the members' actual service dead load axial forces and moments were overestimated by about 20 percent in the design. Regarding moments, data showed that service dead load moments were within 20 percent of those used in the design. The differences between actual and theoretical axial forces and moments for service dead load were attributed to the way the monitoring data was corrected for temperature effects and the possible presence of construction loads on the deck during the pours monitoring.

This case study used limited monitoring and test data to investigate actual stresses at service load levels. It utilized the deck pour monitoring and FE analysis results to estimate axial forces and moments under service total dead load. Analyses of dead load data sets, treating the test and FE results as variables, confirmed with very high certainty the statistical significance of the relationships between these two variables.

Acknowledgments

The authors acknowledge several past and current NYSDOT staff for their contributions to the project. Instrumentation and data collection were conducted by George Schongar and Harry Greenberg. The STAAD III models used in the analysis were developed by Santiago Lopez and Mary Anne Mariotti. The assistance of Mark Norfolk and Hector Hoyos with the data collection and load testing is particularly acknowledged. Dr. Deniz Sandhu performed the statistical analysis. All opinions expressed in this paper are those of the authors and not necessarily of the NYSDOT.

References

- [1] Alampalli S, Frangopol DM, Grimson J, et al. State-of-the-practice of bridge load testing. *J Bridge Eng ASCE*. March 2021;26(3):90. doi:10.1061/(ASCE)BE.1943-5592.0001678.
- [2] Alampalli S, Frangopol DM, Grimson J et al. Primer on bridge load testin. In: *Transportation Research Circular E-C257*. Washington, DC: Transportation Research Board; 2019.
- [3] Hag-Elsafi O, Kunin J, Alampalli S. *Court Street Bridge Monitoring and Load Testing, Special Report 143*. Albany, NY: New York State Department of Transportation; 2006.
- [4] Hag-Elsafi O, Kunin J, Alampalli S. Load testing application for truss bridge design verification: live load testing. *Int J Bridge Eng, Manage Res*. 2024. doi:10.69854/jcq.2024.0009.
- [5] Yannotti AP, Alampalli S, O.C. J, et al. Proof load testing and monitoring of an FRP composite bridge. *Structural Materials Technology: An NDT Conference*; 2000; Lancaster, PA: Technomic Publishing, pp. 281–286.
- [6] Hag-Elsafi O, Kunin J. *Load Testing for Bridge Rating: Route 22 Over Swamp River, Special Report 144*. Albany, NY: Transportation Research and Development Bureau, New York State Department of Transportation; 2006.
- [7] Hag-Elsafi O, Kunin J. *Load Testing for Bridge Rating: Route 32 Over Plattekill Creek, Special Report 146*. Albany, NY: Transportation Research and Development Bureau, New York State Department of Transportation; 2006.
- [8] Hag-Elsafi O, Kunin J. *Load Testing for Bridge Rating: Route 82 Over Sprout Creek, Special Report 145*. Albany, NY: Transportation Research and Development Bureau, New York State Department of Transportation; 2006.
- [9] Hag-Elsafi O, Kunin J. *Load Testing for Bridge Rating: Deans Mill Road Over Hammacrois Creek, J., Special Report 147*. Albany, NY: Transportation Research and Development Bureau, New York State Department of Transportation; 2006.
- [10] Hag-Elsafi O, Kunin J. Monitoring a prestressed concrete box-beam bridge for superloads. *J Trans Res Board TRR 1892 Des Struct*. 2004;1892:126–136.
- [11] Hag-Elsafi O, Albers W, Alampalli S. Dynamic analysis of the bentley creek bridge with FRP deck. *ASCE J Bridge Eng ASCE*. March/April 2012;17(2):318–333. doi: 10.1061/(ASCE)BE.1943-5592.0000244.
- [12] Alampalli S, Hag-Elsafi O, Load testing of bridge FRP applications (Chapter 40). In: *The International Handbook of FRP Composites in Civil Engineering*. Boca Raton, FL: Taylor & Francis Group, Publisher; September 2013:607–622.
- [13] Alampalli S, Hag-Elsafi O, O'Connor J, et al. Use of FRPs for bridge components and methods of performance evaluation. *ASCE Structures Congress 2001*; May 2001; Washington, D.C.
- [14] Hag-Elsafi O, Lund R. Investigation of a cracked hanger plate. *Proceedings of the 2004 Structures Congress—Building on the Past: Securing the Future*; 2004, 1267–1274; Nashville, TN.
- [15] Han F, Prezzi M, Salgado R, et al. *Verification of Bridge Foundation Design Assumptions and Calculations (Joint Transportation Research Program Publication No. FHWA/IIN/JTRP-2020/18)*. West Lafayette, IN: Purdue University; 2020.
- [16] Lin Z, Fakhairfar M, Wu C, et al. *Design, Construction and Load Testing of the Pat Daly Road Bridge in Washington County, MO, with Internal GlasS Fiber Reinforced Polymers Reinforcement. Report No. NUTC R275*. Rolla, MO: Missouri University of Science and Technology. Center for Transportation Infrastructure and Safety; January 1, 2013.
- [17] Raja R, Ali K, Mustafa P, et al. *Implementation Study: Continuous, Wireless Data Collection and Monitoring of the Sagamore Parkway Bridge, Report Number: FHWA/IIN/JTRP-2022/09*. West Lafayette, IN: Purdue University. Joint Transportation Research Program; December 1, 2021.
- [18] Shiu KN, Russell HG. The citation for the article knowledge gained from instrumentation of the kishwaukee river bridge. *PCI J*. October 1983;28(5):32–53. doi: 10.15554/pcij.09011983.32.53.
- [19] Andrew A, Nohemy G, Travis H. Manual for refined analysis in bridge design and evaluation, sponsored by federal highway

- administration office of infrastructure, Report No. FHWA-HIF-18-046; May 2019.
- [20] Bell ES, Gaylord DL, Goudreau A, et al. Bridge instrumentation, testing and modeling for decision making: a case study. *International Symposium Non-Destructive Testing in Civil Engineering (NDT-CE)*, September 15–17; 2015; Berlin, Germany.
- [21] Consolazio GR, Getter DJ, Kantrales GC. *Validation and Implementation of Bridge Design Specifications for Barge Impact Loading*. Gainesville, FL: University of Florida Department of Civil & Coastal Engineering; July 2014.
- [22] *AASHTO Guide Specifications for Strength Design of Truss Bridges (Load Factor Design)*, 1985 (1st edition) including 1986 Interims. Washington, D.C: American Association of State Highway and Transportation Officials; 1985.
- [23] *New York State Department of Transportation Standard Specifications for Highway Bridges, and Provisions in Effect as of April 2001*. Albany, NY: New York State Department of Transportation; 2001.
- [24] *AASHTO Standard Specifications for Highway Bridges, 1996 (16th edition)*, including 1997 and 1998 Interim Specifications. Washington, D.C: American Association of State Highway and Transportation Officials; 1996.
- [25] *Guide Specifications for Strength Design of Truss Bridges (Load Factor Design)*. Washington, DC: AASHTO; 1986.
- [26] Project Design file. *Unpublished, Structures Division*. Albany, NY: New York State Department of Transportation; 2001.